Kaunas University of Technology
Faculty of mechanical engineering and design

Properties of Transparent Wood

Report

Lukas Lenktaitis
Project author

Prof. dr. Darius Albrektas
Supervisor

Kaunas, 2018

Table of Contents

Table of Figures

List of Tables

List of Equations

1 Introduction

Nowadays wood industry is growing rapidly and probably will not be replaceable for ages. Long way ago wood started to be most important building material, hunting tool and helped from freezing. Todays world industry is inconceivable without wood production, most of products we use everyday wood is used. Wood industry creates millions of workplaces all over the world and companies making billions of revenue. And innovation is taking big slices of development - from cutting the wood and providing completed product to customer, no matter is it only timber, complex furniture or building component. Talking about material wood itself has properties and can be distinguish or characterize such very effective and at the same time – cheap material. Wood has ability swell or shrink because due the impact of moisture, can resist high weight load stresses and etc. Nevertheless, today society is curious to create something new to outstand already created products or services. Good example can be transparent wood innovation which has ability to be crystal clear with high optical transparency and what is more incredible – treated wood is able to outstand even steel as a building material. Therefore, transparent wood must be analyzed and approved by advanced testing. This thesis purpose is to treat wood to obtain transparency from majority of types of wood which can be found in nature, test it and from acquired data analyse and conclude what is possibility to use this innovative material of the future‘s prospectives.

2 Specifications of Wood

Wood is one of the most usable material that has various specifications with its excellent physical, chemical and mechanical properties due to the unique of geographical growth and environmental impact. Depending on the types of the wood and geographical zones differences, various woods obtain a plenty variety of molecules structure which creates the lignin with multiple features and different colors (fig.2.1). Wood can be classified into two parts: softwoods and hardwoods, both have its own pros and cons comparing with usability in industry or growth features, nevertheless, they have the same structure of trunk (fig.2.2). Hardwoods are flowering plants, mostly known are oak, maple, ash, teak or walnut, Softwoods are evergreen conifers, such as pine or spruce. For instance, softwoods typically are more porous structure due to growing speed. Softwoods are keeping their "leaves" throughout the year. Hardwoods are known for their denser structure and much bigger density comparing to softwood. Hardwoods shed their leaves during of time in autumn and winter. Structures of the wood can be greatly different, however, the mesoporous structures of all wood which can be found in nature sharing almost the same similarities in the hierarchical structures. Softwoods in their structure contain much more glucomannans, hardwoods – the greater amount of xylans (fig.2.3) [2]. Analyzing the resistant of hardwoods and softwoods, hardwoods have much more stronger immunity for resistant of the decay process than softwoods. However, a good quality hardwood is expensive comparing with softwood and has widely range of usability. In many cases, softwoods and hardwoods are widely used in many industry areas for the same purpose, but emphasizing density properties and how density would be helpful or is it even necessary. However, softwoods are cheaper because of it fast growth and distribution in nature all over the world. About 80% of timber wood production is from softwoods [2], considering that, hardwoods are more common comparing with softwoods. They have a wide range of applications and are been using in furniture where high density is not required,

Figure 2-3. Different types and colors palette of wood . [1]

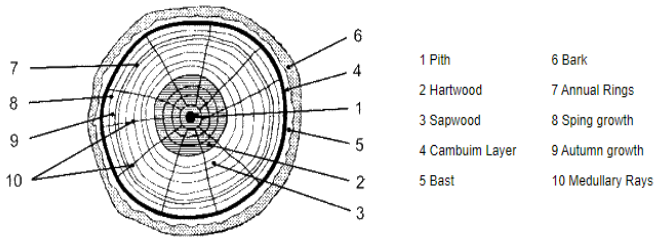

Figure 2-1. Structure of the wood trunk. [4]

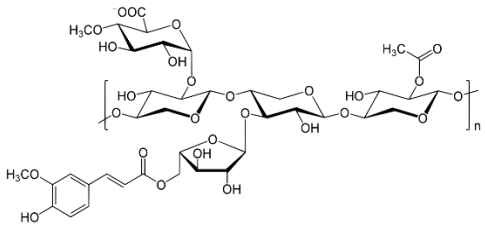

Figure 2-2. Chemical structure of xylan. [3]

building materials and components, medium-density fiberboard (MDF), are widely use in paper production, and much more [2]. For example, pines are one of the most usable and common wood comparing with other woods. As it was mentioned before, hardwoods are much more expensive and because of high density is harder to work with those types of wood, however, higher density means that hardwoods will last longer and will be applicable than softwoods. For this reason, hardwoods are more appreciated and more valued, those types of wood can be found in high quality furniture, flooring are mostly made from hardwoods, decks, and construction that is necessary to last longer period of time. Hardwood and softwood have different addition of, such as, cellulose, lignin and other compositional structures (table 1.1.) which have the impact for their properties. This thesis purpose is to remove lignin which gives impenetrable features, to make wood fully transparent of partly transparent, analyse and compare new obtained characteristics.

	Hardwood	Softwood
Cellulose	42±2%	45±2%
Hemicellulose	27±2%	30±5%
Lignin	28±3%	20±4%
Extractives	3±2%	5±3%

Table 2-1. Compositions of hardwood and softwood. [2]

The differences between those types of wood can be dramatically different. This is even visible properties, such as, broad leaves of hardwood, while the softwoods always are covered by cones and needles. Hardwoods have vessel elements, under a microscope, these elements appear as pores. In softwoods, medullary rays and tracheids produce sap. When viewed under a microscope, softwoods have no visible pores because tracheids do not have pores (shown in fig.2.4). The pores in hardwoods are a lot of what gives hardwood its prominent grain, which is quite different from softwood's light grain [2].

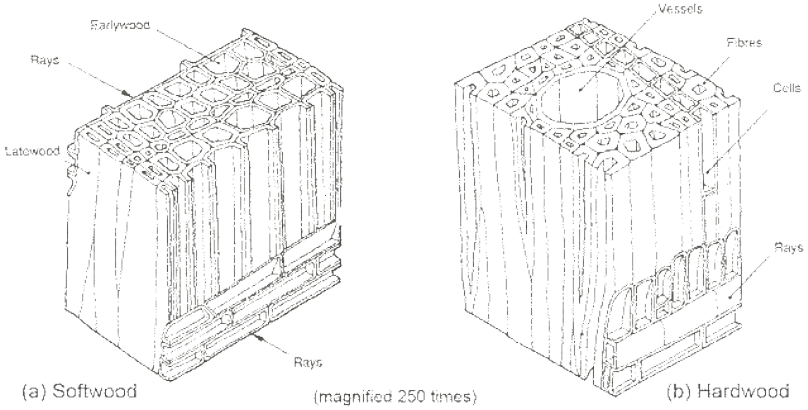

Figure 2-4. Comparison of softwood and hardwood section views. [4]

The most important property of wood is the structural anisotropy, where stands vertical channel, which are aligned. Vertically standing channels helps to pump up water through the trunk and other minerals which are necessary for keeping functionality, supply the leaves for photosynthesis. The wood‘s cell walls which have nano-elementary fibrils, under microscope, can be seen that fibrils are around 3-5 nm of its diameter, and whole structure consist pectin, lignin, and some other elements (fig.2.5). [6]

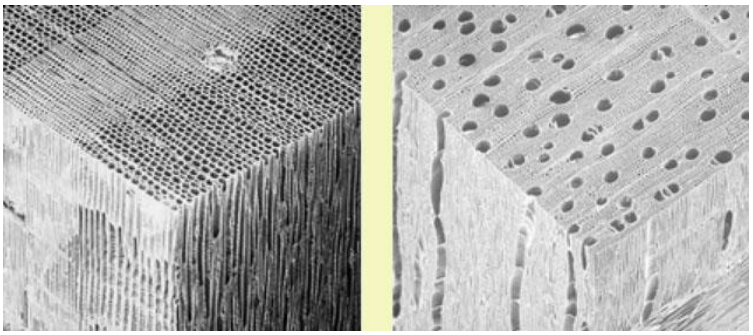

Figure 2-5. Microscope view of wood piece (magnified approx. 50 times). [4]

Interaction among hemicelluloses, cellulose addition, lignin properties and that hierarchical structure make strong bonds between the particles and creates outstanding mechanical properties, which can be found only in the wood structure. Talking about structures of the wood, there can be found cellulose nanofibers which are taking big part of the wood structure, and cellulose nanocrystals, both can be used for energy, in electronics, and widely be valuable due to the nanostructures, strong optical and mechanical properties. Comparing natural wood with transparent wood properties, specifications and composition, transparent wood have been fully made by using and mixing polymers such as epoxy resin. Wood is composed from hemicelluloses and cellulose, both of them are optically transparent and colorless, however, lignin can be characterize such as dark colored structure which is complex as well. The structures such as mesoporous in the wood have scattering light ability in the visibility range (fig.2.6). Consequently, wood obtains nontransparent features with all named structural compositions. [6]

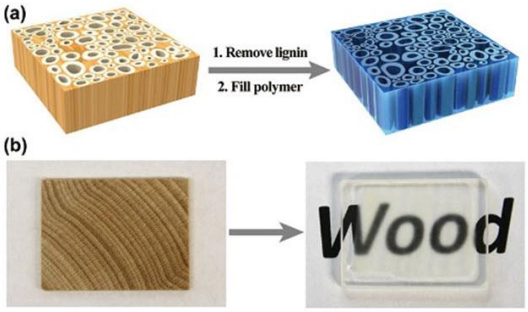

Figure 2-6. Untreated wood vs. treated wood. [6]

3 Transparent Wood Properties

Advanced functionality of wood structures had been obtained by using and combining unique microstructure of the wood. New types of wood such as polymer hybrids or mineral wood hybrids (most known is magnetic wood (fig.3.1)), and advanced composition of bioinspired [6] are changing nowadays world of society thinking of wood applications. Chemical innovations led to obtain new structures of wood which creates new physical and mechanical properties, for example, new tendency is transparent wood which is made via of the bleaching of chemicals, followed by polymer process such as an inclusion. Transparent wood can be used and applied for a variety of applications and realizations in industry or in daily life challenges, in adjustment such as wood furniture to more advanced applications such as building materials, structure compositions, in new cars, in mechatronics and automation machines, optical industry where different transparency levels from all types of materials are required and necessary, or even in electronics [6]. After made transparent wood still maintains its anisotropic composition but becoming crystal clear with high optical transparency. To achieve anisotropic transparent wood composites colored lignin must be removed and filled with index matching polymers to obtain necessary up to 90% optical transparency. Transparent wood is significantly more biodegradable than glass and plastics. For example, fully made transparent wood is shatterproof. Comparing the strength of simple wood and transparent big differences shown up – when testing R-wood and L-wood transparent wood can be ten times stronger when matching nature wood, in the figure 3.2. is shown the differences comparing stresses acting on transparent wood and simple wood. The results shown that nature wood is more vulnerable on acting forces than transparent wood which as a result was more resistant for stresses.

Figure 3-1. Specifications of Magnetic Wood [7].

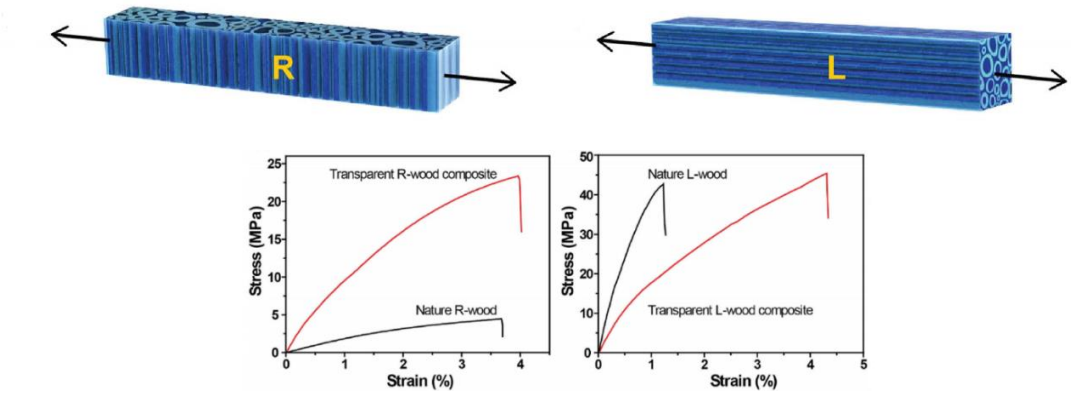

Figure 3-2. Stresses modulus on nature wood and R-Wood and L-Wood. [6]

4 Laboratory Process

The first laboratory work attempt to obtain transparent wood, only radial wood was used, that means, where the original channels in wood align perpendicularly. To complete the process of lignin removal and making transparent wood where the composite displays extraordinary anisotropic optical and mechanical properties it was necessary to investigated the structure, process, properties and relationship in lignin removal and polymer filtration along the lumina which is shown figure 4.1. The resulting anisotropic wood composites keep the original wood micro- and nanostructures, including the aligned cell walls and the inside cellulose fibers [6].

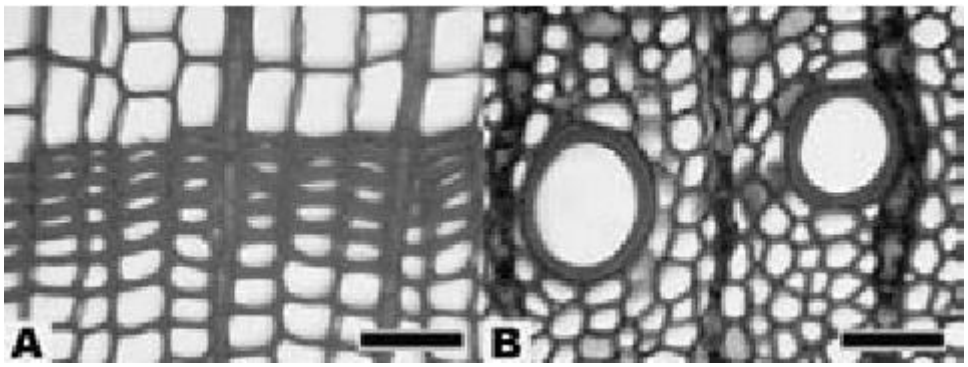

Figure 4-1. (A) – softwood and (B) – hardwood lumina. [8]

The figure 4.2 is shown natural wood and after chemical treatment obtained structure of transparent wood, where the wood plane was cut off perpendicular through channels. Radial cut wood is made by perpendicular cut, in which the wood trunk is radially intersected. Removal of most complex structure in wood – lignin, can be removed without any difficulties, however, it is necessary to maintain and preserve the cellulose structure. After treatment process the lignin can be removed, then the piece of wood becomes transparent, because due the reduced absortion and scattering cause by lackness of the lignin. The lumina after treatment can be infiltrated by epoxy resin for lowering scattering of the light and that allows to obtain high wood transparency. The treatment of longitudinal wood, which can be made by cut wood direction of longitude. The same process of lignin treatment and polymer epoxy resin infiltration is applied as well, however the treatment as whole process will took more time due the length of mass tranportation in the wood

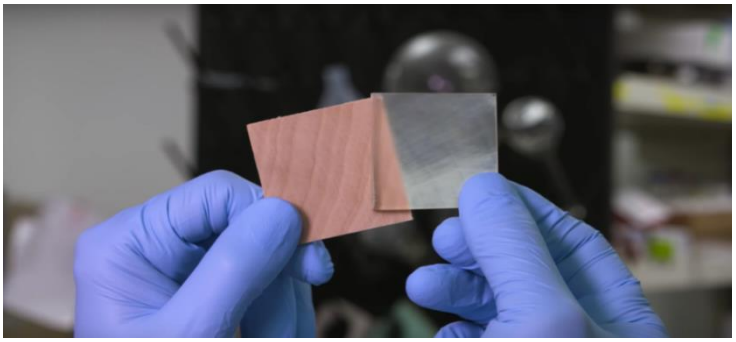

Figure 4-2. Nature wood vs. transparent wood. [9]

structure. Those process can be easily implemented in almost all types of wood with polymer epoxy resin and preservation process in the wood.

In the laboratory work 1-5mm thickness wood were used, most of the pieces were from hardwood such oak, birch, maple, ash and etc. Only pine was used from softwood which was almost 5mm thickness. All pieces were cut with professional equipment and whole surface has the same dimensions of thickness. Chemicals which are widely used in industry were used during this laboratory process and treatment. Firstly, 1 litre of water was pour into stainless pot which should be bigger than 1 litre capacity due the evaporation process. 100 grams of NaOH and 50 grams of Na_2SO_3 were poured into pot with one litre of water and then mixed together. After few minutes of boiling, when water starts to evaporate faster, wood pieces were placed into pot with solution of NaOH and Na_2SO_3. Boiling process was implementing around 10 hours in the first solution, every hour the process was watched and changes were analyzed. After first two hours the wood started to be bleached, however, the solution started be really dark and after other process time the wood did not change substantially only became a little bit more bleached. It can be caused by into one litre of solution placed all wood pieces, which contained too much lignin and the solution started to be too dark to continue the filtration and removal process. Despite of the fact that solution was added few times by about 0.5 litre of water, lignin did not be removed and dark colored consistence left. Most changes and transparent properties were seen in the apple-tree, pear-tree, cobnut, ash and cherry-tree, however, it was not more than ~30% of transparency obtained. Absolute any changes was seen in pine, birch, maple, oak even

Figure 4-5. Oak, birch, maple treatment.

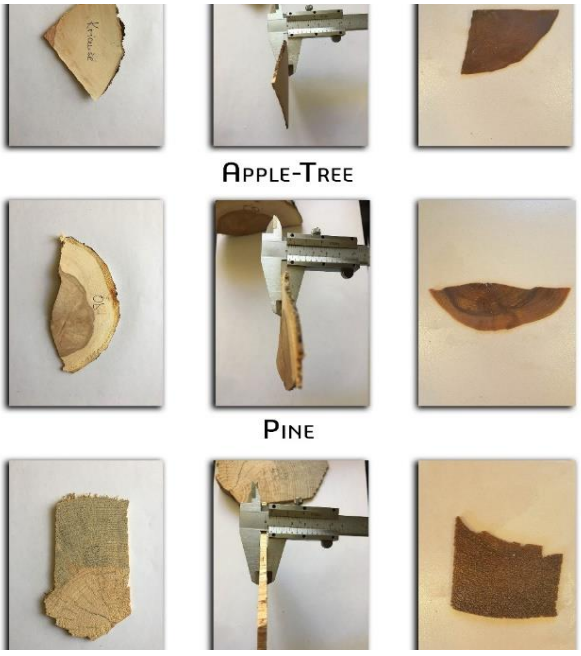

Figure 4-6. Pear-tree, apple-tree, pine treatment.

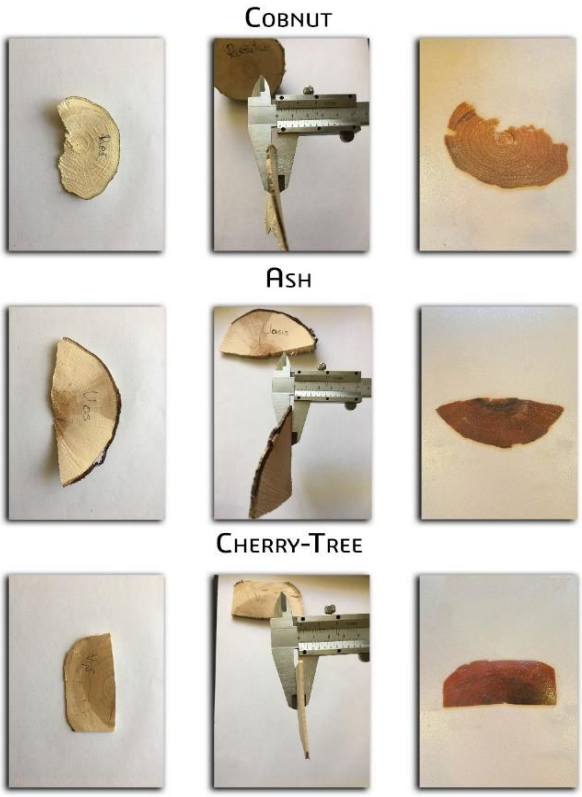

Figure 4-7. Cobnut, ash and cherry-tree treatment.

became darker, due its age. Other lignin of wood pieces was not removed due the size i.e. it was to large (pine), dried up (birch) or due the dark consistency of the solution. Secondly, wood pieces were transferred into pot with H_2O_2 solution for purposes to remove left lignin. Boiling was sat up for two hours, however, due the failure of the first part of the experiment, it has absolutely no impact for wood pieces transparecy. The results can be seen in the figures 4.5; 4.6; 4.7 respectively. Failed experiment in the first part did not allow to continue treatment process with epoxy resin using vacuum. After the second part of the experiment, all pieces were placed into pot with rubbing alcohol for preservation of further processes. During the fourth process of the transparent wood treatment, which was not implemented, the microstruture with aligned channels have to be preserved with epoxy resin, which is most important to obtain mechanical properties, and infiltration process should be implemented. Polymers are infiltrated into pieces of wood towards vacuum, taking wood with epoxy resin (fig.4.8) through around 3 times over 30 minutes. In this vacuum process wood acquires strength properties when all pores are filled with resin. Wood treatment with epoxy substance does not do negative impact to the natural framework of wood structure. During the infiltration process due the bonds interaction between molecules and the cellulose of the wood mechanical properties have been changed and wood becomes optically transparent with new specifitions and properties, which making wood extraordinary material.

Figure 4-8, Crystal clear epoxy resin. [10]

5 Sound absorbtion coefficient

Sounds absorbing production is increasingly, more and more appreciable due very quickly growing industry fields, cities noise, human population growth and other factors. Mostly, valuable sound absorbing materials are used in industry branches such as building engineering, where commonly consist of mineral fibre or glass materials. The vast usage of sound absorbtion materials in the industry markets reduced sound effects on human beings and animals. However, those types of materials are growing concern about the potential risks of health, mostly associated with glass fibre shedding or mineral materials fibre, whereas almost all materials which are used right now are harmful, it provides an opportunity for harmless sound absorbers to be created or developed in industry for the same applications which nowadays is taken by fibre or mineral glass products. Talking about wood which is, as known, from the list of renewable materials and safe for an usage, many types of wood and mixed substances with wood can be apply for sound absorbtion, but new technologicaly treated transparent wood promising more than other materials.

To analyze data of transparent wood and compare it with simple wood, firstly calculations of both wood groups must be measured and calculated according to formulas. To measure sounds absorbtion, longitudinal sounds velocity of wave is required. The velocity of the longitudinal sound wave c (m s^{-1}) can be calculated as follows: []

$$c=\sqrt{\frac{K}{\rho}}=\sqrt{\frac{E}{3\rho(1-2\nu)}},$$

Equation 1 The velocity of the longitudinal sound wave formula [11]

where K is the bulk modulus (N mm^{-2}),

E is the modulus of elasticity MOE (N mm^{-2}),

ν is the Poisson ' s ratio,

ρ is the medium density (kg m^{-3}).

Materials which absorb sound faintly has weak acoustical properties. The porous fabric or materials, for example, wood based or simple wood materials, where impedance Z_c (N s m^{-3}) such as the wavenumber (k_0) is calculated corresponding to density ρ and elasticity's modulus:

$$Z_c = \sqrt{\frac{E\rho}{3(1-2\nu)}},$$

$$k_o = 2\pi f \sqrt{\frac{3\rho(1-2\nu)}{E}},$$

where f is the frequency (Hz). The higher the density of wood, the higher is its elasticity. This also entails a higher impedance (Eq. 2) (Ono and Norimoto 1983 ; K ú dela and Kun š t á r 2011). Simultaneously, at higher medium densities, the acoustic wave velocity is lowered (Eq. 1). That is why wood acoustic properties are also influenced by its porosity Dw and air flow resistivity ξ (N s m -4) (Attenborough 1993 , Wassilieff 1996 , Cox and D ' Antonio 2009). Porosity in the state of absolute dryness is described as:

$$D_w = 1 - \frac{\rho_w}{\rho_s},$$

where ρw is the density in an absolutely dry state (kg m -3), ρs is the density of wood cell wall (ρs = 1500 kg m -3). The flow resistivity ξ can be determined either empirically by laboratory experiments or through analytical calculations. The solution given below was employed by Bies and Hansen (1996) as well as by Cox and D ' Antonio (2009) :

$$\xi = 7.95 \cdot 10^{-10} \left(\frac{\rho^{1.53}}{a^2} \right),$$

where a is the radius of a fiber. Wood fibers, in contrast to glass fibers, can accumulate greater air volume in their inside diameters as well as among themselves. Typical glass fibers in high-quality acoustic panels have approximately 3 – 5 μ m radii and are 3 – 30 mm long (Wassilieff 1996), whereas wood fibers have typically 6 – 20 μ m radii, and their average length is about 3 mm (Po ž

gaj et al. 1997). Hence, they are relatively shorter and wider and more rectangular than cylindrical. Taking into consideration the properties of porous materials, including flow resistivity and porosity, it is possible to calculate their specific impedance and wavenumber (Johnson et al. 1987 ; Champoux and Allard 1991 ; Allard and Champoux 1992 ; Attenborough 1992 ; Champoux and Stinson 1992 ; Allard 1993 ; Wassilieff 1996 ; Wang and Torng 2001 ; Atalla and Panneton 2005 ; Allard and Atalla 2009). Attenborough (1992) demonstrated that density ρ and bulk elasticity modulus K of a porous medium are expressed by the following equations:

$$\rho=\rho_o q^2\left(1-\frac{\tanh(\sqrt{i\beta})}{\sqrt{i\beta}}\right)^{-1},$$

$$K=\gamma P_o\left(1-\frac{(\gamma-1)\tanh(\sqrt{N}\sqrt{i\beta})}{\sqrt{N}\sqrt{i\beta}}\right)^{-1},$$

where:

$$\beta=\left(\frac{6\pi f\rho_o\left(\frac{c}{c_o}\right)^2}{D_w\xi}\right)^{0.5}, \text{ and}$$

Figure 3 presents real Re and imaginary Im components of the normal acoustic impedance on the surface determined experimentally and illustrates their course in the frequency function. It is evident that the highest Re and the lowest Im values were obtained for the 125-Hz frequency. Only in the case of T04, T05, T06, T07, T16, T13, and T15 wood composites, the real part of the surface impedance exhibited the highest values at 250 Hz frequency. From a practical point of view, acoustic properties of materials for frequencies between 250 Hz and 3 kHz are interesting because this band includes musical sounds and human speech. With this regard, the lowest Re values (from 1.01 to 4.36) were recorded for T14 and T17 panels confirming their considerable capability for sound absorption. For T04 and T05 panels, high Re values (from 13.36 to 255) are typical, which limits possibilities for their practical application. Sound absorption capabilities are illustrated in F igure 4a , from which it is obvious that T17 panels have the best acoustic absorbability for all frequencies, i.e., 0.06, 0.24, 0.56, 0.64, 0.5, and 0.36, respectively. In the case of initial frequencies ranging from 125 Hz to 500 Hz, also the following traditional chipboards have relatively high absorption coefficients: T10 (0.04, 0.06, 0.06) as well as T15, T11, T14, T16, and T13. With regard to frequencies ranging from 1 kHz to 2 kHz, high absorption coefficients were also recorded for the following panels: T07 (0.10, 0.25), T05 (0.09, 0.25), T06 (0.10, 0.24), and T03 (0.11, 0.23). In the case of the highest frequency of 4 kHz, high absorption capabilities of 0.64, 0.40, 0.36, 0.28, and

0.23, respectively, were found for the following panels: T14, T01, T17, T12, and T03. It is evident that the best sound absorption capabilities can be found in wood-based materials characterized by low density of surface layers and high porosity. This regularity applies, in particular, for the frequencies from 125 Hz to 500 Hz. Honeycomb panels with a paper core better absorb sound at 1 kHz – 2 kHz frequency. For the 4 kHz frequency, panels with large external surface irregularities possess the most advantageous properties. They are obtained by appropriate forming (T14), gluing of comminuted particles (T12, T17), or finishing by veneer of rough structure (T01, T03). Figure 5 illustrates the effect of composite density and sound frequency on its absorption by the examined wood-based materials. This figure corroborates the regularity that high sound absorption

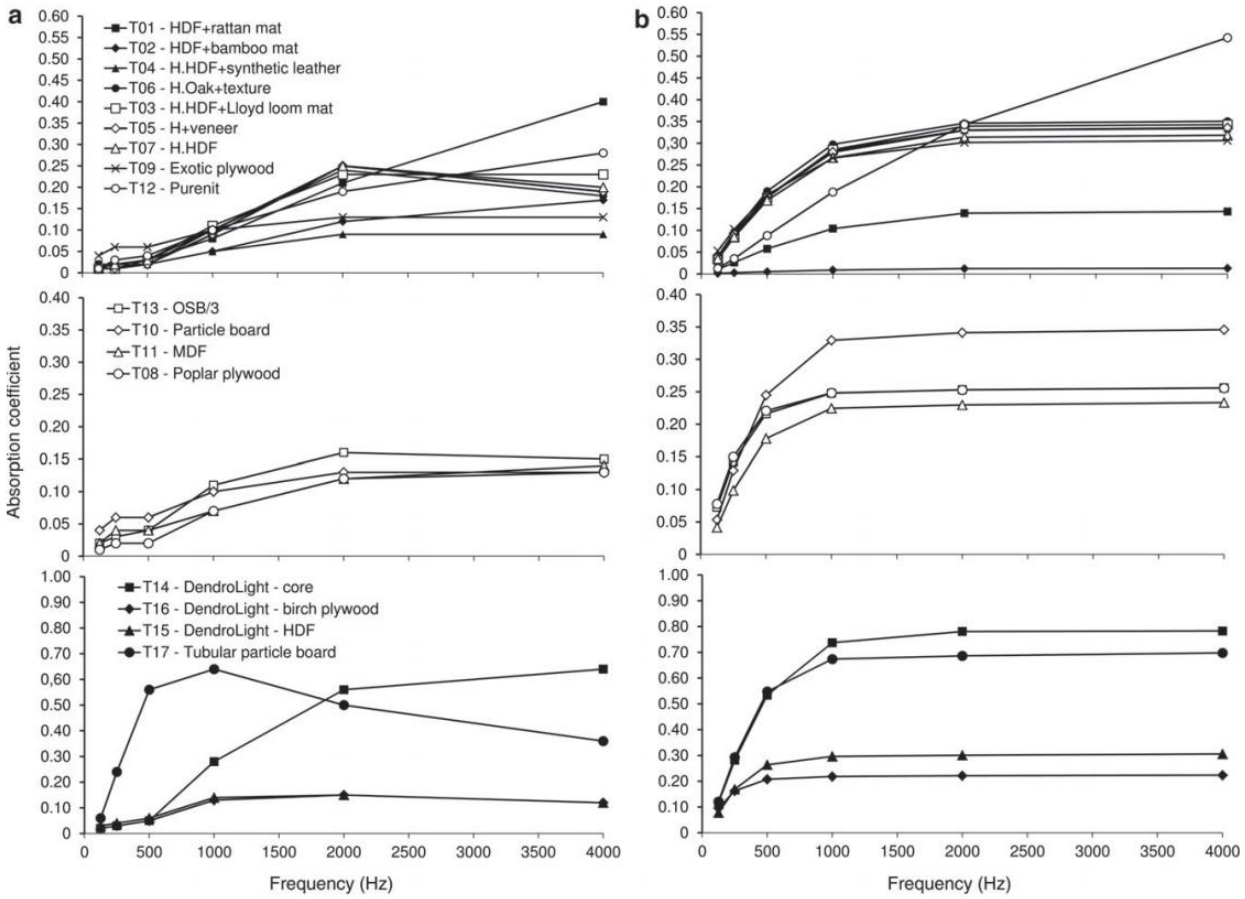

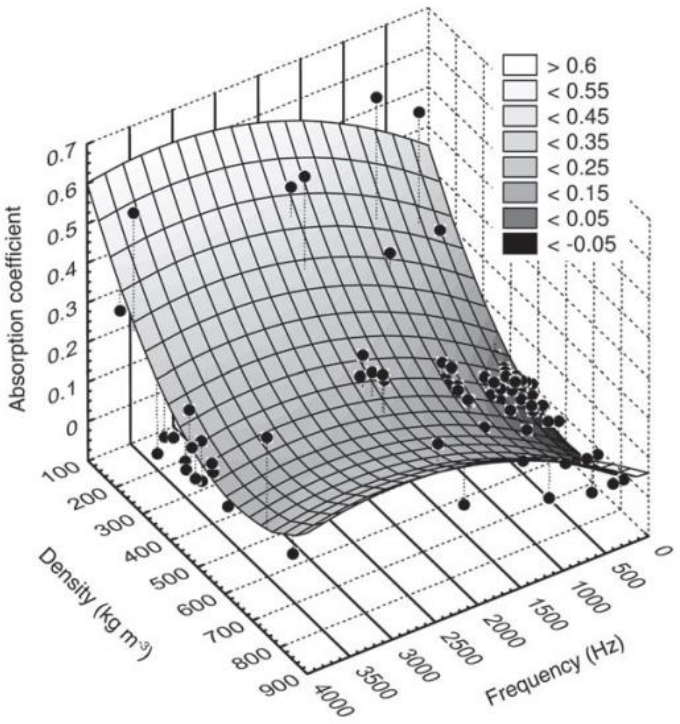

Epoxy Resin

Compared to natural fibers, the sound absorption property of their reinforcing composites apparently decreased. Natural fibers possess excellent sound absorption property by themselves whereas the hollow lumen and air space would be significantly diminished. The resin would occupy some effective volume of airflow and the cavities between fibers and inside lumens were compressed by the pressure added during the process of composite manufacturing. Figure 10 shows the sound absorption properties of epoxy resin and it can be seen that the sound absorption behavior of the resin system is very low. Additionally, the sound absorption property largely depends on the frequencies of sound wave. The higher the frequency, the shorter the sound wave length and the longer the propagation path of sound wave in the composites. Therefore, more dissipation of sound energy happens in the composites. This explains why natural fiber composites have the best sound absorption performance at high frequencies.

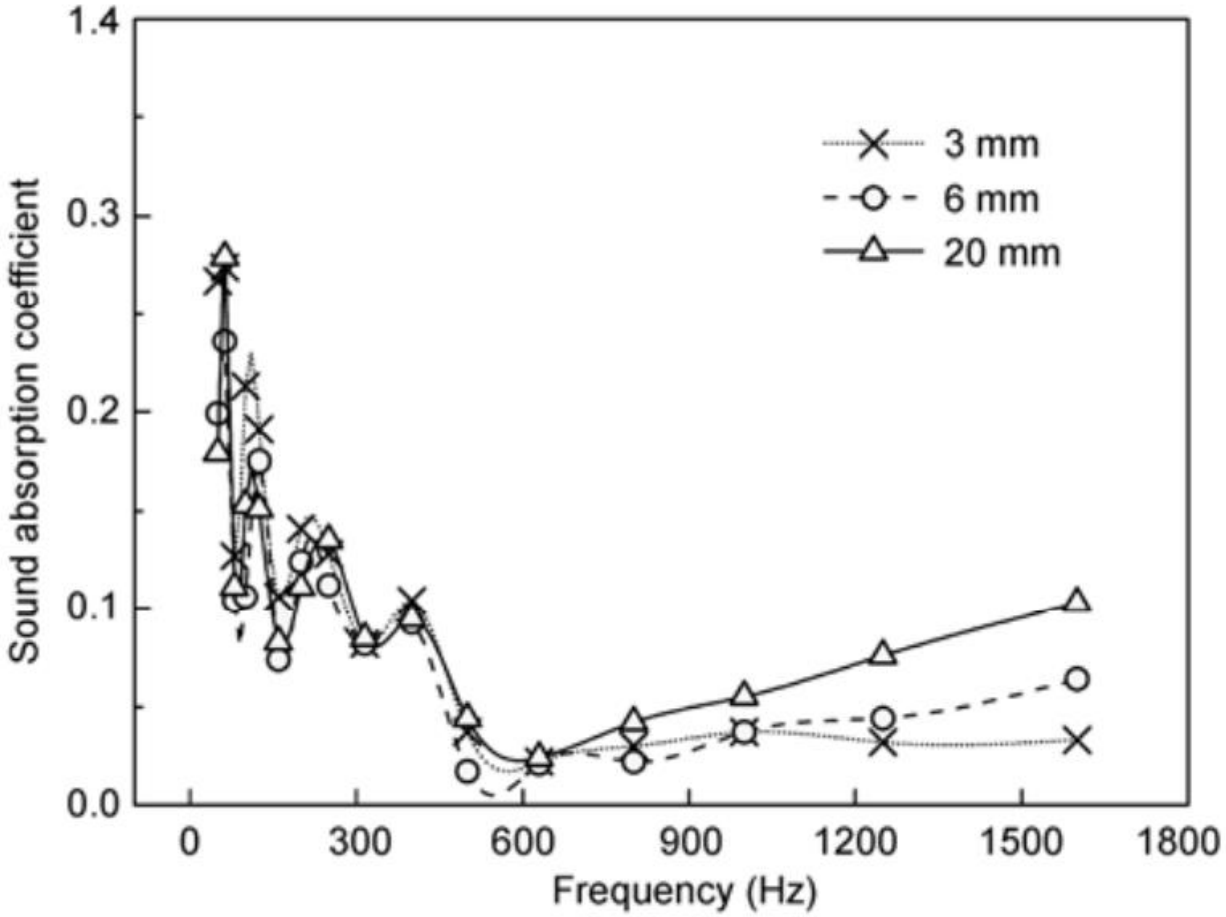

6 Luminescent Transparent Wood

Functional light conversion layers containing active fluorescent materials are necessary components in many devices. The most straightforward example would be the common white light-emitting diode (LED), where blue emission from a GaNbased diode is partially converted to red and green emission using a phosphor-rich layer. Most commercial devices rely on rare-earth-based phosphors,[1] however quantum dots (QDs) have also been considered.[2] These nanosized light emitters are usually dispersed in homogeneous silica[3] or polymer[4,5] layers in close proximity to the excitation LED. Thus their size is relatively small, and the concentration of fluorescent centers high. Typically, they are combined with an additional passive diffuser component to minimize the influences of viewing angle and to achieve uniform illumination, such as using a patterned structure,[6] porous layers,[7,8] or films with embedded microparticles[9,10] So far, white LEDs have been thought of as distinct localized illumination sources, which are not part of the constructions or materials they

illuminate. In this letter we present the preparation of a conversion layer realized by the virtue of the natural porous wood structure of the newly developed transparent wood material.[11] In contrast to thin layers of transparent nanocellulose paper,[12] this delignified wood represents a 3D porous bulk structure suitable as reinforcement in load-bearing components. Matching the refractive indices of the pore-filling polymer and the cellulose fibers ensures optical transparency.[11,13,14] Here the pore-filling monomer methyl methacrylate (MMA) was enriched with luminescent QDs before embedding it into the cellulose fiber network for subsequent polymerization. We show that QDs reveal no signs of optical degradation upon this transition, where different nanocrystal materials were tested. Under blue/UV excitation the resulting 2 × 2 × 0.2 cm slabs exhibited diffused red and green luminescence arising from the embedded Si and CdSe QDs, respectively. Structures containing Si QDs offer a unique opportunity to evaluate scattering losses because the optically active Si QDs have negligible reabsorption at the emission wavelength.[15] The scattering strength of the luminescence was found to be dependent on the wood fiber direction, consistent with the original wood structure being preserved. High scattering values (i.e., up to ≈ 10 dB cm−1) indicate strong suppression of the total internal reflection required for emitted light propagation. This luminescent transparent wood nanocomposite offers interesting possibilities for applications, which can benefit from its unique structural and optical properties. Examples would be furniture for general lighting or luminescent solar concentrators for building integration,[16–19] where the proven mechanical strength of this transparent wood[11] is a clear advantage. The nontoxicity and material abundance of Si QDs further enables sustainable and large scale manufacturing of this new luminescent material. Silicon QDs were synthesized upon processing of hydrogen silsesquioxane by thermal annealing.[20] The resulting nanocrystal-containing silicon oxide composites were treated with ethanolic hydrofluoric acid to extract hydride terminated nanocrystals. It was followed by surface passivation using well-established hydrosilylation procedures described elsewhere.[21,22] Toluene dispersions of the resulting alkyl-passivated Si QDs feature external photoluminescence quantum yields in the range 30%–60%.[23] Samples used here had peak positions in the red (720 nm) and near infrared (870 nm) spectral range. To demonstrate the possibility of incorporating different types of QDs commercially available CdSe/ZnS core/shell quantum dots with green emission (540 nm, Evident Technologies) were used. The wood template was obtained by delignification of wood veneer (balsa, Ochroma pyramidale, purchased from Wentzels Co. Ltd, Sweden) with dimension of 2 × 2 × 0.2 cm to remove the main light-absorbing component.[24] The thickness direction of the veneer is the tangential direction of the cross-section of the tree stem. Specifically, wood veneer was treated using 1 wt% of sodium chlorite (NaClO2, Sigma-Aldrich) in acetate buffer solution (pH 4.6) at 80 °C. The reaction was

stopped when the wood appeared almost uniformly white. The delignified samples were washed with deionized water and kept in water until further use. Prior to polymer infiltration, wood samples were dehydrated upon sequential exposure to ethanol and acetone with each solvent exchange step repeated three times. The MMA monomer was pre-polymerized before mixing with QDs. The prepolymerization was completed by heating the MMA at 75 °C for 15 min with 0.3 wt% 2,2′-azobis (2-methylpropionitrile) followed by cooling to room temperature. This process yielded a mixed solution with MMA monomers and oligomers. Subsequently, the delignified wood template was fully vacuum-infiltrated with the prepolymerized MMA/QDs solution in a desiccator under house vacuum with pressure of 13 mbar. Finally, the infiltrated wood was sandwiched between two glass slides, wrapped with aluminum foil, and heated in an oven at 70 °C for 4 h in ambient atmosphere (Figure 1). The rightmost image in Figure 1 shows the red-emitting Si QDs containing transparent wood composite with letters beneath clearly visible under ambient light. Absolute photoluminescence (PL) quantum yields, luminescence, and absorption spectra were measured in a home-built instrument based on an integrating sphere. The selected excitation wavelength was 440 nm (6 nm linewidth) filtered by a monochromator after a laser-driven Xe-lamp.[23] To evaluate the scattering strength, the QD luminescence was collected from the sample edge using a 10× objective lens of an inverted microscope and detected by a CCD camera. The excitation spot (≈1 mm diameter) was focused on the sample front surface from a 405 nm laser diode and scanned across it using a mirror system. For PL mapping a color camera (Zeiss, AxioCam) was used and the image was taken from the sample edge with a 100× objective lens after a long pass 635 nm filter under broad spot excitation from the 405 nm laser. For structural characterization cross-sections of QD wood samples were investigated using a field-emission scanning electron microscope (SEM, Hitachi S4800) operating at a low acceleration voltage of 1 kV and in the secondary electron collection regime. The cross-section was prepared by fracturing a freeze-dried sample after cooling in liquid nitrogen and polishing with 1–10 µm sand paper. SEM analysis reveals that the QD-rich polymer fully infiltrates pores of the delignified wood without large cavities visible at this magnification (Figure 2a). To gain insight into the distribution of QDs throughout the wood template, PL mapping was performed. This imaging reveals a uniform distribution of emission centers (Figure 2b) with signal intensity varying within 10% across the image (noticeable grooves appearing in the image are the results of surface polishing). Embedding QDs in polymer matrices can lead to deterioration of their optical properties due to particle aggregation,[25] however we have demonstrated that Si QDs encapsulated in acrylic glass retained their optical properties (i.e., peak position, quantum yield, and lifetime).[26] The fabrication procedure employed to prepare the present hybrid materials differs slightly and includes a mixing of

a prepolymerized MMA with QD solution, an infiltration into the cellulose fiber network followed by a final heat treatment. To interrogate any potential impact of this synthetic approach on the QDs optical performance, we monitored the luminescence quantum yield. To reduce the measurement error related to limited absorption, a high initial concentration of QDs in toluene was used (>0.1 wt%). The initial sample of Si QDs in toluene solution showed a broad emission peak at 870 nm (particle average diameter ≈6 nm) and 35%–40% quantum yield. A QD-free wood reference sample (left) and the wood slab with these QDs (right) are shown in Figure 2c (inset). The emission and absorption spectra of the QD wooden slab are provided in Figure 2c. Indeed, neither the luminescence spectrum nor the quantum yield was impacted upon incorporation of the QDs into the polymer or wood template. Quantum dots are known to be more resistant to bleaching than, e.g., organic dyes, and we found no changes in Si QDs optical properties when embedded in pure polymethyl methacrylate (PMMA) for months.[26] Unlike previously described samples in Figure 1, which remain optically transparent after QD impregnation, the slab in Figure 2 is only partially transparent for the visible range and has a slightly brown color. While the Stokes shift is still significant for these relatively large Si QDs, their absorption markedly increases already in the green/blue spectral range (Figure 2c). For the samples of Si QDs with emission peak position closer to the visible range (red Si QDs in Figures 1 and 4) the wood transparency is largely unaffected by QD incorporation even at similar concentration levels. The large Stokes shift in that case makes smaller Si QDs absorption-free throughout most of the visible range.[26] To evaluate the light scattering ability of this wood/polymer/QD hybrid the QD-based luminescence was collected at the sample edge by varying the excitation spot position. The schematic representation of this experiment is shown in Figure 3a (inset). The use of Si QDs with an appreciable apparent Stokes shift ensures the measured extinction is mainly contributed by scattering. It is known that light-emitting states of these Si QDs remain largely of indirect bandgap character[27] leading to long (≈μs) luminescence lifetimes[28] and strongly suppressed reabsorption at the emission wavelength.[15] For an ideal slab with no scattering and reabsorption the collected intensity does not depend on the source position[29] (dotted line in Figure 3a). The fraction of light emitted from the slab edge is then defined only by the cone with a critical angle ≈42° (for the polymer/air refractive index contrast of ≈1.5/1). Above this angle the emitted light experiences total internal reflection inside the slab. In practice, inhomogeneities inside and on the slab surface lead to scattering outside of this cone. This is evident from the reference sample, where Si QDs were embedded into glass (blue line in Figure 3a). Here a fused silica slab was implanted with Si+ ions to create a nonstoichiometric glass and then annealed to form red emitting quantum dots.[30] The measured loss values for this sample are typical for real systems of QDs embedded in transparent

matrices, such as glass or PMMA, which are of the same refractive index.[19] The losses can be minimized by more uniform and defect-free preparation of the host matrix and its surface, which is important for applications as large-area luminescent solar concentrators. For quantum dots embedded in wood, the luminescence intensity reaching the edge becomes much lower. When the light propagation direction is parallel to the fibers (edge is perpendicular to fibers), the scattering losses amount to ≈3 dB cm−1 (black line in Figure 3a). In the case of perpendicular propagation relative to the fiber direction (edge is parallel to fibers) the losses become an order of magnitude larger, reaching ≈10 dB cm−1 (red line in Figure 3a). These directiondependent losses clearly demonstrate the anisotropic structure of the wood template preserved in the QD nanocomposite. Figure 3b reveals this highly aligned hollow cell system of the wood. The cell wall thickness is around 1 µm, while the pore size ranges from around 10 to 60 µm with vessel pores being in the order of hundred microns. The fiber lengths are in the range from hundreds of micrometers up to a millimeter. When light propagates perpendicular to the fiber direction, more scattering centers are encountered at the cell wallPMMA interfaces compared with propagation parallel to the fiber direction. So only a small fraction of the emitted light reaches sample edges, yet there is negligible reabsorption in the sample. As a result, luminescence is mainly scattered out of plane, as explicitly shown in Figure 4a,b. Here we took photoluminescence photographs of the red Si QD glass and the red Si QD transparent wood samples under laser diode excitation (spot in the middle). The glass sample, as a planar waveguide, directs the light emission to the edges. In contrast, QD transparent wood displays a diffused luminescence in the whole chip, leading to a planar lighting instead. This is an attractive property in general lighting, where light diffusers are often needed to generate spread, uniform illumination. To demonstrate the possibility of incorporating different types of QDs in the transparent wood, CdSe QDs were also successfully embedded resulting in green luminescence. Figure 4c shows a photograph of CdSe QD transparent wood together with a PMMA envelope around it. When pumped from the PMMA edge (bottom center on the image) diffused luminescence in the CdSe QD transparent wood becomes visible. At the same time a fraction of the emission light is guided to the edges inside the PMMA layer. This proves that wood structured QD transparent composites provide a combination of a light diffuser with the conversion layer. A visibly better light propagation parallel to the fiber direction is also noticeable in this sample under the used in-plane excitation. Although CdSe QDs are known to exhibit some toxic effects,[31] they were selected here simply to show universality of the method for different QD material systems. The origin of this diffused luminescence is mainly due to the small interface gaps between wood and PMMA, although optical inhomogeneities in cellulose fibers and in the PMMA also contribute. Though PMMA was fully infiltrated into the wood structure, interface

gaps still exist in the composite due to nonoptimized chemical compatibility between cellulose and PMMA (Figure 4d). Additionally, PMMA shrinkage during polymerization contributes to the formation of interface gaps. Although these gaps are favorable when diffused scattering is desired (such as luminescent building or furniture and planar lighting), we could possibly further tune the scattering strength through wood surface modification. This can improve the interface quality and reduce scattering. Transparent wood with such haze control has potential applications ranging from planar lighting with highly diffused luminescent scattering to luminescent solar concentrators, where the waveguiding regime is favorable for light harvesting at the edges. We also note that a plywood configuration can be used to achieve more isotropic luminescence scattering. This nanocomposite material is expected to be less prone to degradation caused by moisture, microorganisms and UV radiation than original wood thanks to near-complete pore filling with PMMA, acting as an efficient barrier against liquid, and due to the removal of lignin, which is the main component subjected to UV-degradation in wood. In conclusion, luminescent transparent wood combining optical and load-bearing functions was successfully fabricated by infiltration of a wood template with QD-rich MMA. No signs of optical degradation were detected upon this transition, indicating good compatibility of a transparent wood matrix for QD encapsulation. The wood structure introduced strong scattering, resulting in diffused luminescence from embedded quantum dots, which is advantageous for planar light sources and luminescent building construction elements or furniture. Surface modification of the wood cell wall will help to tune the light scattering properties of this new material, making it attractive for a wider range of applications.

7 Transparent wood

The rapid development of optoelectronics technology is making the possibility of flexible displays a soon-to-be-available reality. Among these display technologies, the organic light-emitting diode (OLED) has received a lot of attention because of its attractive features for display applications. However, commercially available OLEDs are fabricated on glass substrates. Although flexible plastics are expected as alternatives to existing glass substrates, no prospect of actually using plastics has yet emerged due to its high coefficient of thermal expansion (CTE). Foldable plastics, in particular, have extremely large CTEs, exceeding 200 ppm K1 . As multilayers of different materials are deposited on the substrate by thermal processes, the thermal cycling induces a mismatch in the CTEs of the layers, subjecting them to strain and eventual cracking [1]. In order to restrict the thermal expansion, some reports have proposed the fabrication of transparent nanocomposites made of plastics reinforced with bacterial cellulose (BC) 50 nm wide nanofibers [2–4]. Due to the low thermal

expansion of cellulose nanofibers, these new materials offer an extremely low coefficient of thermal expansion [2], an indispensable property for display substrates, of just 4–6 ppm K1 . Because BC nanofibers with a cross section of 10 50 nm2 are virtually free from light scattering, high transparency was obtained even at high fiber contents such as 60– 70 wt.% [2,3]. Clarity of the substrate is important especially for bottom-emissive OLED displays [1]. The foldable and ultralow CTE (4 ppm K1) transparent BC nanocomposites were produced recently by reinforcing a low Young's modulus transparent resin with 5 wt.% of BC nanofibers [4]. But unfortunately, widespread industrial use of BC would probably require the development of expensive large-scale fermentation technology. The cost of the cellulose nanofibers is expected to be lowered by the use of more abundant resources than BC. Many researchers have been studying the extraction of cellulose nanofibers from biomass materials [5–12]. Recently, the extraction of uniform, 15-nm-wide nanofibers from wood powder was attained by a grinding treatment [13]. The use of cellulose nanofibers from wood, which represents the majority of plant resources, is the most effective and practical application to cellulose nanocomposites intended for OLED substrates. In this study, therefore, we investigated the properties of wood– cellulose nanocomposites with special attention to the elastic modulus of matrix resin and then evaluated the potential application of these samples into display substrates. As a result, we succeeded in producing optically transparent wood–cellulose nanocomposites with the performances of both low thermal expansion and low Young's modulus. Ultimately, we accomplished depositing an electroluminescent layer on flexible, low-CTE and transparent wood–cellulose nanocomposites. 2. Experimental 2.1. Sample preparation The starting material for the nanofibers was wood powder from Douglas fir (Pseudotsuga menziesii) sieved through a 60 mesh sieve.

The extractives of wood were removed using ethanol and toluene (v/v = 1:2) for 6 h in a Soxhlet apparatus. Afterwards, lignin in the sample was removed using an acidified sodium chlorite solution at 70 C for 1 h, and the process was repeated 5 times [14]. Last, the sample was treated in 5 wt.% potassium hydroxide solution at room temperature for 12 h, and at the same concentration at 80 C for another 2 h in order to leach hemicelluloses. Due to these treatments, the lignin content of the wood decreased to 0.1 wt.% [15] and the acellulose content comprised more than 85% [13]. After washing them with distilled water, the water in the sample was replaced by acetone. To reduce the hygroscopicity of cellulose fibers and to improve the resin impregnation, fibers were acetylated based on the results of previous reports [16–18]. The sample was placed in a mixture of 500 ml toluene, 400 ml acetic acid, and 2.5 ml 60% perchloric acid. Then the necessary quantity of acetic anhydride was added and stirring was maintained for 1 h at room temperature. The DS (degree of substitution) value

of the cellulose derivative was calculated from the C content in the elemental analysis data. Thus, acetylated samples with DS 0.5 were obtained. After acetylation, the samples were washed with distilled water and passed through a grinder (MKCA6–3; Masuko Sangyo Co., Ltd.) at 1500 rpm. The acetylated wood–cellulose nanofibers slurry was dispersed in water at a fiber content of 0.2 wt.%. One hundred-twenty milliliters of the water suspension was vacuum filtered using polyterafluoroethylene membrane filter (0.1-lm mesh), producing a thin mat 90 mm in diameter. The dried sheets were impregnated by dipping them in matrix acrylic resins under a reduced pressure of 0.09 MPa for 12 h. To producematrix resin having various elastic moduli, ABPE10, an acrylic resin with a low Young's modulus (ShinNakamura Chemical Co., Ltd., refractive index: 1.536 at 590 nm and 20 C) and TCDDMA, one with a high Young's modulus (Mitsubishi Chemical Corp., refractive index: 1.532 at 590 nm and 20 C) were mixed at different proportions. Nine types of matrix resin were prepared: ABPE (pure ABPE10), 8A:1T (ABPE10 and TCDDMA mixed at a rate of 8:1), 4A:1T (4:1), 2A:1T (2:1), 1A:1T (1:1), 1A:2T (1:2), 1A:4T (1:4), 1A:8T (1:8), and TCDDMA (pure TCDDMA). Afterwards, the resin-impregnated sheets were cured by UV light. The acetylated wood–cellulose nanocomposites were 90–100 lm thick, and the fiber contents, calculated based on the oven dry weights of dried sheets and the acetylated-wood nanocomposites, were around 35– 40 wt.%. Neat acrylic resin sheets 100 lm in thickness were also prepared under the same curing conditions. 2.2. Measurements 2.2.1. Light transmittance Regular light transmittances were measured at wavelengths from 200 to 1000 nm using an UV–vis spectrometer with an integrating sphere 60 mm in diameter (U-4100, Hitachi High-Tech. Corp.). 2.2.2. Tensile test Tensile moduli were evaluated using a universal materials testing machine (3365, Instron Corp.) for samples 20 mm long and 3 mm wide at a crosshead speed of 1 mm/min with a gage length of 10 mm. The displacement was measured by movement of grips. Five specimens were tested for each set of samples. 2.2.3. Coefficient of thermal expansion (CTE) The CTEs were measured by a thermomechanical analyzer (TMA/SS6100, SII Nanotechnology Inc.). Specimens were 25 mm long and 3 mm wide with a 20 mm span. The measurements were carried out during elongation with a heating rate of 5 C/min in a nitrogen atmosphere at a load of 3 g. The CTE values were determined at 20–150 C in the second run. 2.3. Organic light-emitting diode (OLED) displays OLED material was fabricated on the cellulose nanocomposites according to the method by Yoshida et al. [19] as follows: (1) Smoothing Layer: Spin coating, (2) SiON Barrier Film: Sputter deposition, (3) Anode: Sputter deposition and patterning, (4) Organic Layers: Vacuum deposition, (5) Cathode: Vacuum deposition, (6) Passivation Film: Chemical vapor deposition. 3. Results and discussion Light transmittance versus wavelength for ABPE, 1A:1T and TCDDMA are shown in Fig. 1. At a wavelength of 600 nm, all nanocomposites

transmitted 82–85% of the light, including Fresnel's reflection. The degradation in light transmittance caused by nanofiber reinforcement was only 6–9% of the original value. The Young's modulus of the nine types of the neat resin sheets and composites are shown in Fig. 2a, and the typical stress–strain curves of ABPE, 1A:1T and TCDDMA resins and their nanocomposites are shown in Fig. 2b. The Young's modulus and tensile strength of all resins increased drastically by reinforcement with 35– 40 wt.% cellulose nanofiber. Furthermore, the result for TCDDMA demonstrated clearly that brittle resin materials became ductile by reinforcement with wood–cellulose nanofiber networks, revealing how the nanofiber networks suppress crack propagation in the matrix resin. It must be emphasized that these nanocomposites possess suitable mechanical properties for continuous roll-to-roll manufacturing. The CTEs of the neat resin that had a low Young's modulus were higher, as expected from general plastic materials (Fig. 2a, Table 1). However, the CTEs of the nanocomposites showed a completely opposite trend. A clear tendency of decreasing CTE values was observed for nanocomposites with the matrix resin of lower Young's modulus in an almost linear mode. For example, the CTE of the TCDDMA nanocomposite was 28.5 ppm K1 , while that of the ABPE nanocomposite was 12.1 ppm K1 . It is believed that the induced thermal stresses are small enough to be almost completely constrained by the rigid cellulose nanofiber networks when the Young's modulus of the matrix resin is low [4]. A low CTE, typically less than 20 ppm K1 of the substrates, is desirable to match the thermal expansion of the substrates to the deposited OLED layers [1]. The wood–cellulose nanocomposite using resin with a low Young's modulus could offer these thermal properties. Ultimately, we manufactured OLED material on the cellulose nanocomposites. We succeeded in depositing an electroluminescent layer on flexible transparent wood–cellulose nanocomposites using resins with lower rates of ABPE than 2A:1T (Fig. 3). However, it was impossible to fabricate OLED panels on the 4A:1T, 8A:1T and ABPE nanocomposites because cracking occurred on the substrate's surface during the process. Examination of the nanocomposite surface by CCD camera revealed the presence of an extra resin layer without reinforcement. This might occur because the samples were made by dipping the dried cellulose sheets in the matrix resin, thereby covering the cellulose as well as impregnating it. Consequently, strain and cracking arose from the mismatch in CTE between the extra resin layers, which have larger CTEs, and the OLED layers. If this assumption is correct, fabricating an OLED layer on foldable wood–cellulose nanocomposites with extremely low CTE such as 12.1 ppm K1 could be possible by removing these extra resin layers. In summary, we accomplished the fabrication of an organic light-emitting diode on flexible, low-CTE and optically transparent wood–cellulose nanocomposites. At the same fiber content, the nanocomposites using lower Young's modulus matrix resin exhibited lower CTE values

than using higher Young's modulus matrix resins. It led to the development of nanocomposites with a very low CTE while having high flexibility and ductile properties. Furthermore, because these nanofibers are derived from wood, production of the nanocomposites can be undertaken at a commercial scale. It is an expectation of the authors that these nanocomposites will open up many possibilities for the application of OLEDs in flexible, transparent displays.

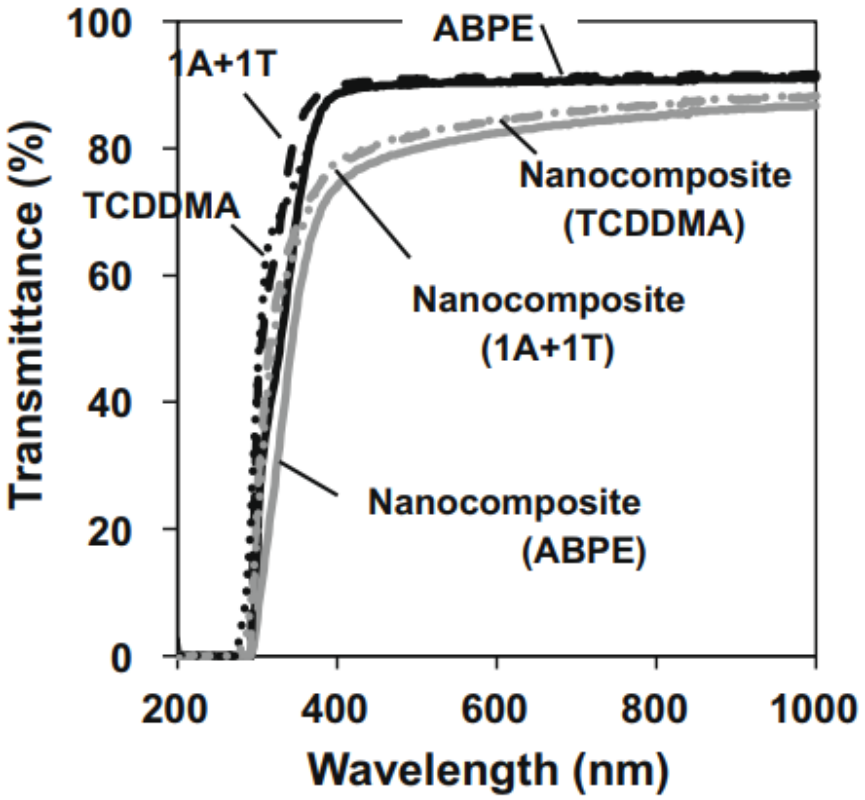

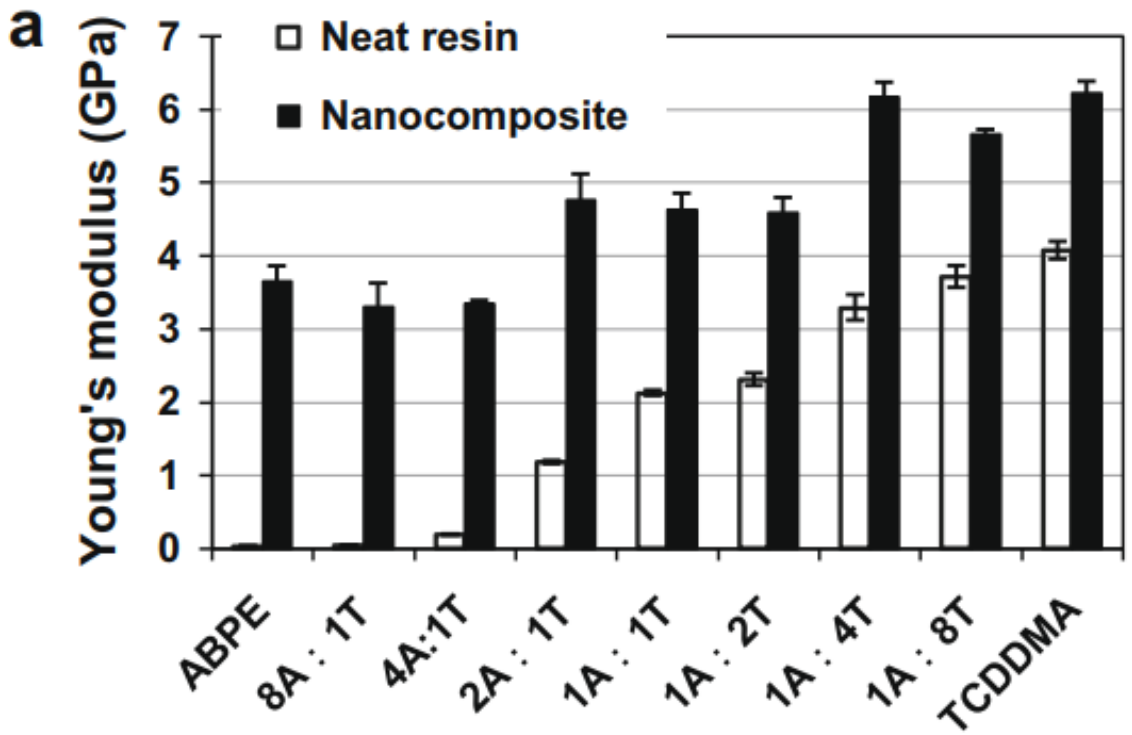
a
Young's modulus (GPa)
0
1
2
3
4
5
6
7
Neat resin
Nanocomposite
ABPE
8A : 1T
4A:1T
2A : 1T
1A : 1T
1A : 2T
1A : 4T
1A : 8T
TCDDMA

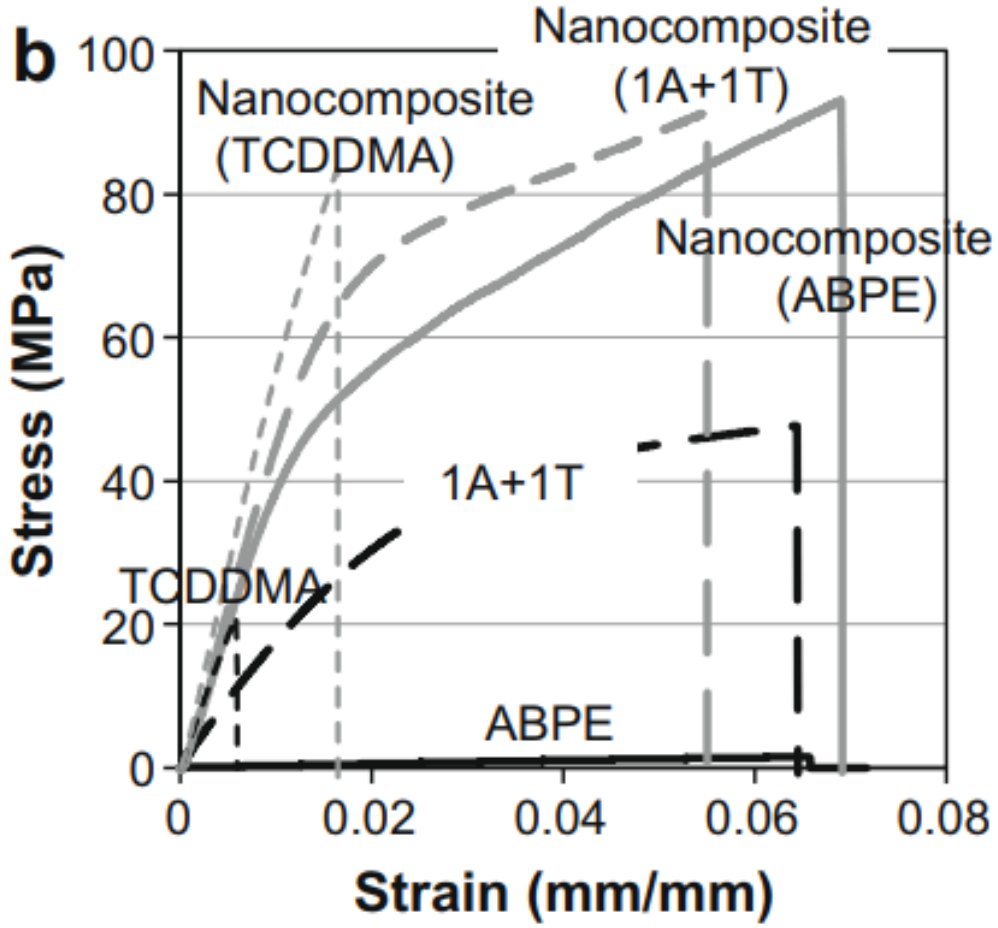
b
Stress (MPa)
0
20
40
60
80
100
Nanocomposite
(TCDDMA)
Nanocomposite
(1A+1T)
Nanocomposite
(ABPE)
1A+1T
TCDDMA
ABPE
0
0.02
0.04
0.06
0.08
Strain (mm/mm)

8 Frequences of Transparent Wood

In the figure 6.1 is shown the SEM photography with low magnification and higher magnification of untreated beech wood which is named BW, delignified wood which is DW, and obviously transparent wood which is shorted as TW. The SEM images show a clear presence of the three-dimensional structure of the wood for all the samples [12]. In addition, the SEM photography of the beech wood (BW) emphasize the complex structure of lignin with aligned pores of the wood. Comparing delignified wood to the untreated wood, conclusion can be made that the delignified wood after long delignification process, has retained the three dimensional system and structure with exact complexity of the wood. Talking about that complex structure, it shows that pores are continuously aligned with parallel to the main axis of the wall's cells which means that the consistence of cellulose is still remained, no matter of a long process of the delignification. Moreover, images of the SEM where the transparent wood (TW) is shown, it can be seen that the polymers are not only fully fulfilled with epoxy resin inside the wood, but bonds between cell walls are strongly and rigidly bonded. Taking in advanced by observations of materials, it expected to obtain very strong interaction with polymer between cell walls that can be either mechanical or chemical property. Moreover, void spaces that could be observed are mainly due to the shrinkage of methyl methacrylate by volume after polymerization at the interface between the cell wall of the wood and polymer. In the diagram 1 is shown the FTIR analysis of the beech wood which is untreated, transparent wood, and delignified wood in samples. As it shown, the absorption

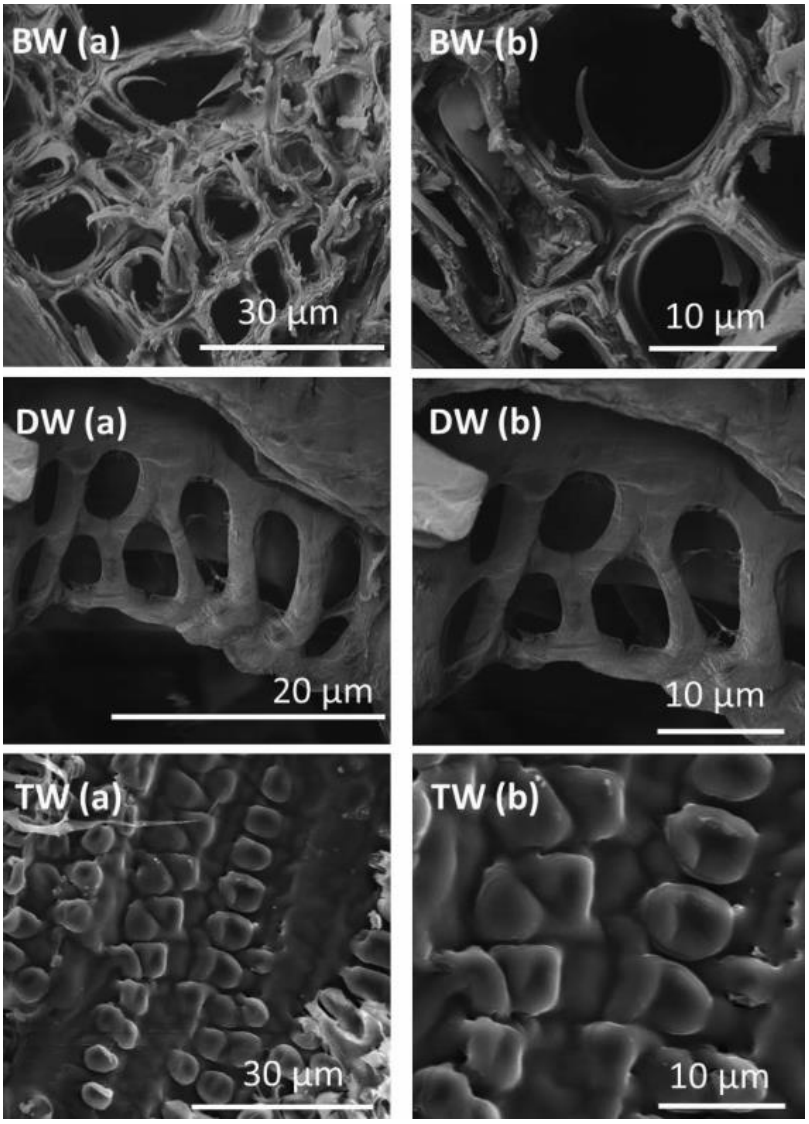

Figure 8-1. SEM images of untreated beech wood (BW), delignified wood (DW), and transparent wood (TW) at (a) low magnification, (b) high magnification.

intensity is over 3500 cm^{-1} and it is decreased from untreated beech wood to the transparent wood. This downfall of the intensity is occured due to the lowered number of hydroxyl substance of the material. Thus, because of the presence of the vinyl monomer, MMA is carrying an ester group and an unsaturated C-C double bond [12]. In polymerization process, the matrix of the wood's structure gets into the ester through mechanism of the polymerization, which is free-radical. Defining bonds between particles, structure is compounded between polymer and the matrix of wood due formation the PMMA wood. In addition, the highest peak is formed at around 1700 cm1 and 790 cm^{-1}. 890 cm^{-1} is result which was obtained due to the polymer's carbonyl group, where polymer is infiltrated into the matrix of wood that is obtaining a strong chemical bonds as it shown in the SEM photography of the transparent wood as it presented in the diagram 4. Moreover, the peak at 1200 cm^{-1} was obtained for the untreated wood due the lignin. Despite of the lignin groups, the highest points at 3390 cm^{-1} and 2950 cm^{-1} are presented in the diagram 1, which are defined as O - H absorption of stretching and C - H bands of absorbtion, respectively, for hemicellulose and cellulose. Comparing the delignified wood to the untreated wood, the delignified wood indicates the non-existence of lignin groups which shows in the further results that the wood's lignin is almost removed from the structure.

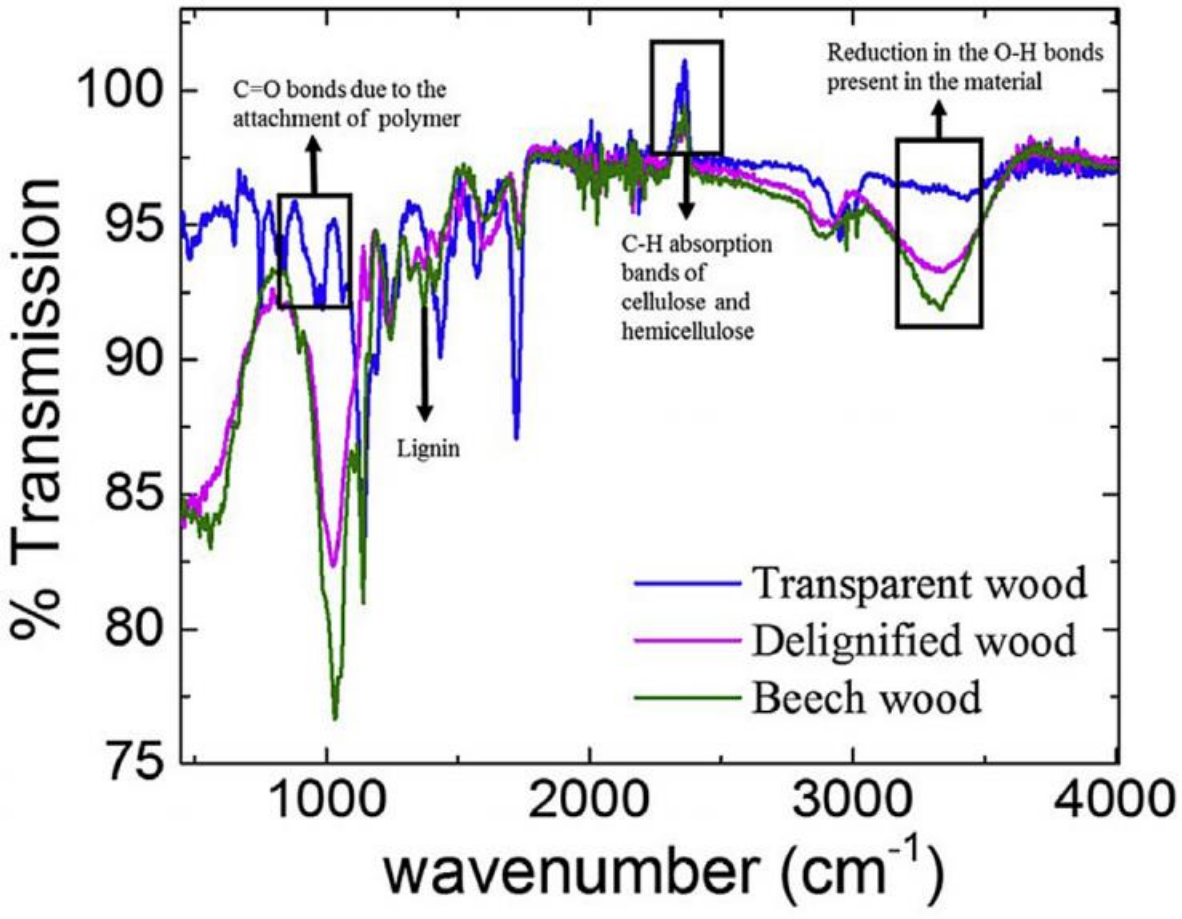

Diagram 1. FTIR spectra of beech wood, delignified wood, and transparent wood over a range of 400

cm———————————————————1 to 4000 cm^{-1}[12]

In the diagram 2 Measurements of the optical specifications are given for the optical transmittance measurements for untreated beech wood, delignified wood, and transparent wood of varying thickness (0.3 mme0.7 mm) over a wide wavelength range of 300 nme850 nm [12]. Concluding the results, it can be seen that the beech wood is absolutely not transparent. That feature occurs because of addition of hemicellulose which absorbing almost all amount of the light, lignin and cellulose. As a result, transparent wood's transmission has reached over 70% in 500 nm wavelength and more.

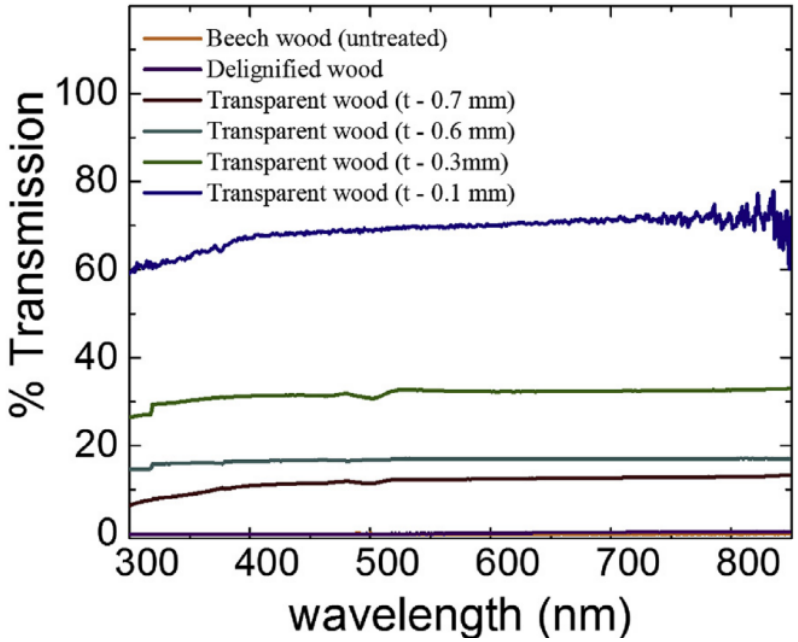

Diagram 2. UV-Visible optical transmittance measurements of beech wood, delignified wood, and transparent wood of varying thickness (0.1 mme0.7 mm) over a range of 300 nme850 nm. [12]

Furthermore, when the thickness is decreasing of the transparent wood, the transmission in the percentage as well are changing. For example, in the diagram 2 is shown that when the thickness of the sample increases, transmission's amount decreases. The best results was obtained of 0.1 mm thickness of transparent wood, respectively, transmittance of 70%, comparing to the lowest transmittance of 0.7 mm thickness of transparent wood – 15% of transparency was obtained. This variation in the amount of transmittance is due to the fact that when light gets transmitted, attenuation takes place which is due to the absorption and scattering [12]. It can be explained as a higher thickness, possession of the light takes a longer pathway which is a result of the lower transmittance. In the future, it is expected that the transparent wood will lead of development of the innovative transparent windows of wood which will have the much higher transmittance comparing with glass or plastics windows which are dominating right now in the market. With transparent wood properties and betterment of technological implementation during the process of purification it will lead to new

adjustment into new building materials with unseen properties.

In the diagram 3 is presented the measurements of optical haze of varying thickness transparent wood with in comparison with PMMA. The highest results of optical haze was around 49% from 0.7 mm of thickness of the wood sample which was over 400 nm. Respectively, the sample of a thickness around 0.3 mm indicate a haze of barely 18%. Main importance is to combine and control both – the haze and the transmittance percentages to implement it in various projects and applications. For instance, in display applications, low haze such as 1% - 15% is the requirement to obtain substance without glare. In different circumstances, more than 15% of a haze is considered to be more beneficial for systems and structure materials in solar cells. The higher percentage of haze the higher amount of improvement in the light absorption efficiency will be increased in the path of light which is transmitted on the area of the active layer for solar cells. As a result, there can be an enhancement in the short circuit current density of solar cells [12]. As a result on this theory, transparent wood with a high haze in purification process will be able to play a huge role in optimization in solar cell industry and its applications.

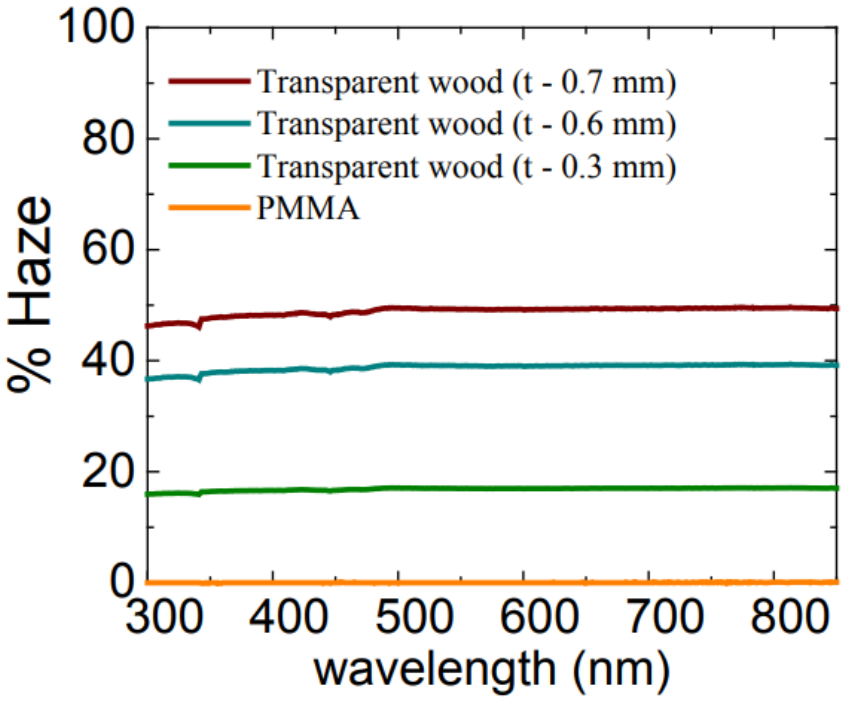

Diagram 3. UV-Visible optical haze measurements of beech wood, delignified wood, and transparent wood of varying thickness (0.3 mme0.7 mm) over a wide wavelength range of 300 nme850 nm. [12]

9 Mechanical Properties

Transparent wood has strong mechanical properties as well. In the diagram 4, is shown the comparison of the mechanical property of stress-strain curves for different materials – resin impregnated transparent wood, delignified wood, beech wood, and PMMA. After testing the results was obtained and conclusions can be made, that the transparent wood is more way stronger with an elastic modulus is of 2.5 GPa. Comparing other types of woods such as the delignified wood whose elastic modulus is 2.1 GPa, transparent wood is stronger more than 0.4 GPa. Taking in comparison beech wood of 1.52 GPa and PMMA with an elastic modulus of 2.3 GPa, conclusion can be made that transparent wood is the strongest of all compared materials. The low elastic modulus was acquired of the delignified wood which has lackness of strong bonds of the hydrogen binding around wood cells and whole structure itself. Besides of shown calculations, the wood. which is transparent, is much harder with hardness of 23 HRC when the beech wood has little less than transparent wood - 21 HRC, The delignified wood hardness was recorded with 12 HRC. Analyzing obtained results can be easily conclude that transparent wood which is mix with wood and clear epoxy resin was much more improved due betterment with interaction inside wood's cell walls and polymers structure which can be seen in the FIGURE Moreover, delignification of the wood results in enhancement of the specific surface area from 9.8 m2 /g to 18.9 m2 /g as determined by BET measurements. This is betterment and facilitation into impregnation areas of PMMA for the pores in the wood's structure. It made strong and gave toughness to bonds of hydrogen which is formed across walls of the cellulose in addition with the hydroxyl substance and polymer groups it creates stronger connections. Moreover, this PMMA cellulose bonding inside itself is expected to improve significantly not only hardness or toughness, but even other mechanical (tensile strength) and non- mechanical properties such as air permeability on the material. [12]

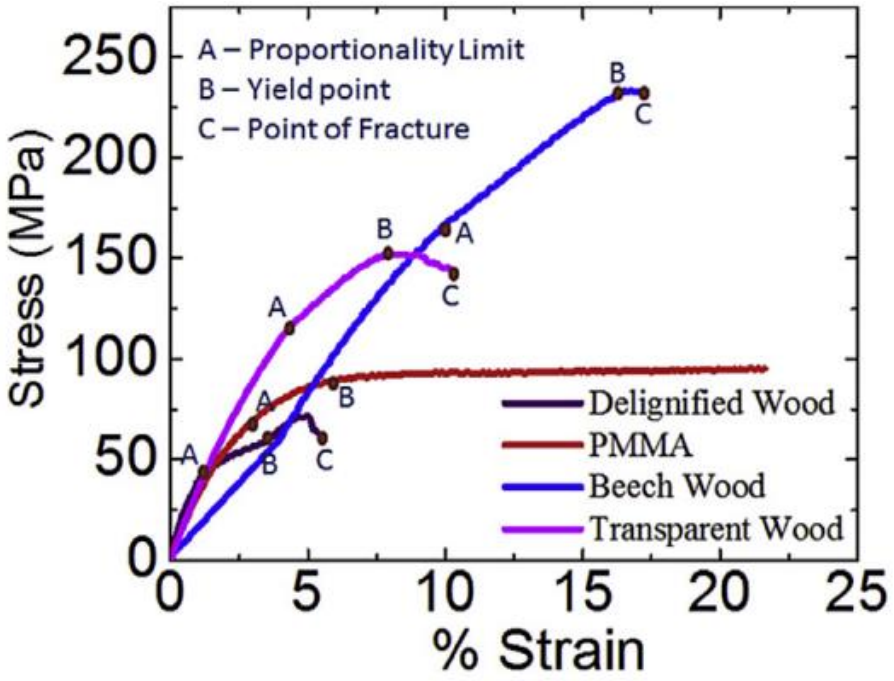

Diagram 4. Stress v/s Strain relationship of beech wood, delignified wood, transparent wood and PMMA. [12]

10 Conclusions

Optical clear transparent wood is one of those innovation which can change materials science future forever, and open new opportunities for other new materials. Transparent wood has chances to overcome similar materials because of forces which this material can handle and optical transparency feature. It is innovative, extraordinary material that has to enter the materials market and be one of the most usable organic material. However, to obtain necessary transparecy is not quite easy, it requires time and only thin pieces can be made transparent, that means there is no possibility to overtake other material such steel in todays innovation level

.

11 References

1. *Different Types and Colors Palette of Wood and its Applications*. [seen 2018-05-05]. Available on https://www.jambartechawards.com/
2. *Differences, Comparison, Properties of Softwood and Hardwood*. [seen 2018-05-10]. Available on https://www.diffen.com/difference/Hardwood_vs_Softwood
3. *Properties and Structural Analysis of Xylan's Molecules in Nature.* [seen 2018-05-10]. Available on https://www.wikiwand.com/en/Xylan/
4. *Wood Specifications and Comparison of Softwood and Hardwood*. [seen 2018-05-10]. Available on https://www.boeingconsult.com/tafe/mat/timber/howtreegrows-oh.htm/
5. *Guidance of Experiment - Transparent Wood Treatment* [seen 2018-05-18]. Available on https://www.instructables.com/id/transparent-wood/
6. *Highly Anisotropic, Highly Transparent Wood Composites by Mingwei Zhu. (2016).* Available on http://onlinelibrary.wiley.com.scihub.cc/doi/10.1002/adma.201600427/full
7. *New Type of Wood Application – Magnetic Maple Knife Rack*. [seen 2018-05-20]. Available on https://www. etsy.com/listing/459636502/tiger-maple-knife-rack-magnetic-knife /
8. *Wood Lumina Specifications of Softwood and Hardwood*. [seen 2018-05-22]. Available on https://www.researchgate.net
9. *Transparent Wood Properties and Specifications after Treatment*. [seen 2018-05-22]. Available on https://www.futuresplatform.com/blog/transparent-wood
10. *Crystal Clear Epoxy Resin Coating Hardener For Wood Treatment*. [seen 2018-05-22]. Available on https:// https://promarinesupplies.com
11. *Sound absorption of wood-based materials*. [seen 2018-11-22]. Available on https://www.sciencedirect.com/science/article/abs/pii/0003682X96000138
12. *Fabrication and characterization of transparent wood for next generation smart building applications*. [seen 2018-11-22]. Available on https://www.sciencedirect.com/science/article/abs/pii/S0042207X1630728X

12 Appendices

Property	Oak (southern red)	Pine (red)	Spruce (Engelmann)
Density (gr/cm^3)	0.59	0.46	0.35
Humidity ratio (%)	12	12	12
Modulus of elasticity (E_T/E_L)	0.082	0.044	0.059
Modulus of elasticity (E_R/E_L)	0.154	0.088	0.128
Modulus of elasticity (G_LR/E_L)	0.089	0.096	0.124
Modulus of elasticity (G_LT/E_L)	0.081	0.081	0.120
Modulus of elasticity (G_RT/E_L)	0.009	0.011	0.010
Poisson's ratio (μ_{LR}) *	0.350	0.347	0.422
Poisson's ratio (μ_{LT}) *	0.448	0.315	0.462
Poisson's ratio (μ_{RT})*	0.560	0.408	0.530
Poisson's ratio (μ_{TR})	0.292	0.308	0.255
Poisson's ratio (μ_{RL})	0.064	0.080	0.083
Poisson's ratio (μ_{TL})	0.033	0.050	0.058
Modulus of rupture in static bending (kPA)	75,000	76,000	64,000
Mod. of elasticity in static bending *EL* (MPa) *	10,300	11,200	8,900
Mod. of elasticity in static bending *ET* (MPa)*	845	493	525
Mod. of elasticity in static bending *ER* (MPa) *	1,586	985	1,140
Modulus of rigidity (*GLR*)*	917	1,075	1,104
Modulus of rigidity (*GLT*)*	834	907	1,068
Modulus of rigidity (*GRT*)*	89	123	89
Impact bending (mm)	660	660	460
Compression perpendicular to grain (kPa)	42,000	41,900	30,900
Compression parallel to grain (kPa)	6,000	4,100	2,800
Shear parallel to grain (kPa)	9,600	8,400	8,300
Tension parallel to grain (kPa)	3,500	3,200	2,400
Side hardness (N)	4,700	2,500	1,750
Adhesive shear strength (MPa)	8,000	8,000	8,000

Table 12-1. Mechanical properties of wood.